

# Experimental Confinement Studies Beyond ITER

Akihide FUJISAWA

National Institute for Fusion Science, Oroshi-cho, Toki 509-5292, Japan

(Received 5 January 2009 / Accepted 16 May 2009)

The advantages of stellarators are discussed with an emphasis on the high density limit more than 10 times higher than that of tokamaks with the equivalent magnetic field strength. The comparison between stellarators and tokamaks in the light of the new paradigm of plasma turbulence and zonal flows is presented to propose a new optimization principle of magnetic field configuration. The roles of low-temperature devices should be recognized for further understanding of the plasma confinement even in the era of burning state plasmas

© 2010 The Japan Society of Plasma Science and Nuclear Fusion Research

Keywords: tokamak, stellarator, density limit, zonal flow, flow damping, principle of configuration optimization, low temperature device

DOI: 10.1585/pfr.5.S1005

## 1. Introduction

The research aiming at realizing a sun on the earth has been carried out for more than fifty years. The efforts have advanced the physics of magnetically confinement along with the development of fusion technologies. A wide variety of the toroidal magnetic field confinement have been tested, such as tokamaks, spherical tokamaks, stellarators including many kinds of configurations (*e.g.*, heliotron, heliac, and helias), reversed field pinches, bumpy torii, magnetic mirrors, and so on.

At present a device, ITER, is being constructed to realize a tokamak plasma in burning state. This is because the tokamak is the leading concept of the magnetically confinement fusion, where a number of records, in fact, have been made. The followings have been achieved for instance; the ion temperature of 40 keV and the fusion product of  $1.5 \times 10^{20} \text{ m}^{-3} \cdot \text{s} \cdot \text{keV}$  in JT-60U, the electron temperature of 20 keV in ADEX-U, the confinement time of 1.2 s and the stored energy of 17 MJ in JET. The spherical tokamak, with an extremely low aspect ratio of less than 2, has achieved the highest  $\beta$  of  $\sim 40\%$ , together with high plasma confinement due to the large capacity of plasma current [1].

The studies of other magnetic configurations, however, should still continue to be carried out to demonstrate their own advantages or individualities that can avoid the undesirable characteristics of standard tokamaks. For example, the nominal currentless characteristic of stellarators makes the steady state operation of the discharges much easier. The comparative studies of various concepts should be necessary to optimize magnetic field configuration in terms of confinement, energetic particle behaviour etc., and to realize an advantageous device adopting the merits of different concepts in terms of the economic and steady state operation. This paper will discuss several physical

and experimental topics for obtaining a better solution of a magnetically confined fusion device in future.

## 2. Advantages of Stellarators

### 2.1 High density operation of stellarators

The simple coil geometry of tokamak requires the internal plasma current to produce rotational transform for the plasma confinement. The resultant confinement field has an axisymmetric nature to serve the good confinement property, however, the external current drive is mandatory for steady state operation. The toroidal current can be the cause of the disruption to determine the density limit, since the radiation density limit (or the Murakami limit [2]) should be too high to be met in the modern clean plasma with well-conditioned wall. The empirical formula to describe the density limit of the modern tokamaks is known as the Hugil-Greenwald limit [3], which is expressed as

$$\bar{n}_{G,\text{limit}} (10^{20} \text{ m}^{-3}) = \frac{I_p}{\pi a^2}.$$

where  $I_p$ (MA) and  $a$ (m) represent the plasma current and the minor radius, respectively. It has been experimentally supported that the density limit in the tokamak plasma should be bounded by the violent deterioration of the confinement [4].

On the other hand, the density limit of stellarators is known to be described by an empirical law, termed Sudo scaling [5, 6] which is approximately written as

$$\bar{n}_{S,\text{limit}} (10^{20} \text{ m}^{-3}) = 0.25(P_{\text{abs}}B/(aR^2))^{0.5} \propto \sqrt{P_{\text{abs}}B}.$$

where  $R$ (m),  $P_{\text{abs}}$ (MW) and  $B$ (T) represent the major radius, the absorbed power and the magnetic field, respectively. This expression suggests that the stellarator density limit should be deeply associated with the condition of radiation balance with the absorbed heating power, the radi-

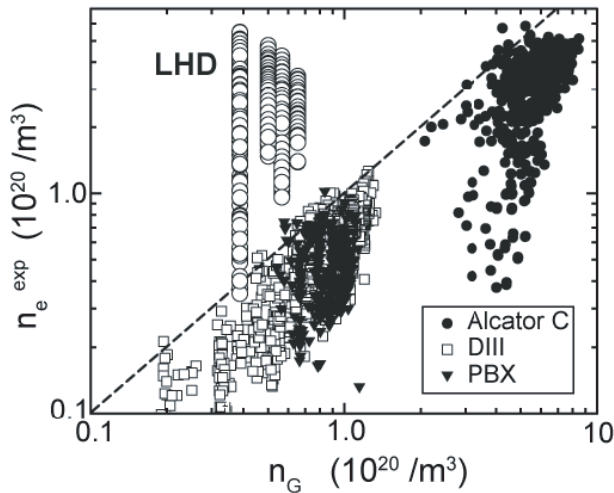


Fig. 1 Comparison between operational density in LHD and several tokamaks. The obtained density is plotted as the function of the corresponding Greenwald density. The achieved density in LHD is obviously ten times or much more higher than the Greenwald density (Courtesy of Prof. H. Yamada).

ation should be proportional to the square of density, i.e.,  $P_{\text{abs}} \propto n_e^2$ .

It has been also well known that the density limit of stellarators is well above the Greenwald limit. Figure 1 shows an example of the high density limit of the LHD heliotron, compared to the Greenwald limit of tokamaks. Moreover, the stellarators do not show any violent plasma behavior around the density limit, while the tokamak operation near the density limit leads the plasma to disruptions.

## 2.2 Behavior near density limit in stellarators

A number of scenarios have been reported for stellarator plasmas around the density limit. In addition to the behavior like apparent radiation collapses, the rapid decrease in the stored energy and the following recovery, called *breathing*, is found around the density limit of the NBI plasmas in LHD [7] and W7-AS [8], when the magnetic field strength is properly selected at a fixed heating power.

In CHS an interesting behavior suggesting a transition is observed at the density limit. Figure 2 shows the temporal evolutions of line-averaged density, radial power, stored energy, and so on. The plasma is sustained with electron cyclotron resonance (ECR) heating with rather low power of  $\sim 100$  kW. In this case the line-averaged density increases gradually to reach a density limit. At the beginning of the exponential growth of radiation, a concomitant decrease with the stored energy is observed without any significant increase in MHD activities in a Mirnov coil signal. Just after the radiation reaches its maximum, the rapid decrease of radiation occurs and the radiation relaxes into a constant value. The potential signal observed with an

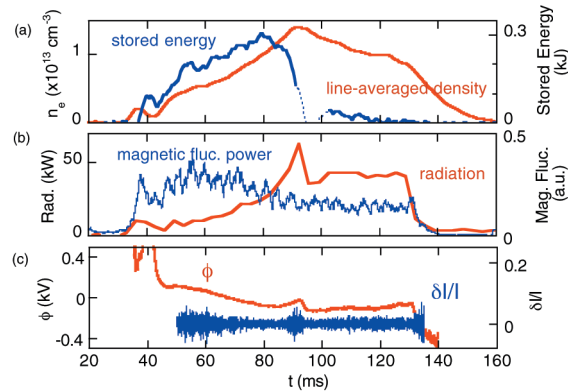


Fig. 2 Behavior of the ECR-heated CHS plasma at  $\sim 100$  kW. Time evolutions of (a) line-averaged density, stored energy, (b) radiation, magnetic field fluctuation power less than 50 kHz, (c) potential, and density fluctuations measured with HIBPs. The density limit is achieved or a transition happens at  $t \approx 90$  ms.

HIBP also shows a rapid decrease in potential simultaneously with the radiation.

According to the observation, the plasma behavior before and after the density limit (or maximum) point can be regarded as a transition from a state with high stored energy (or temperature) to the other one with extremely low stored energy (or temperature). On the other hand, the density fluctuations observed with an HIBP, or intermittent activity of density, show a rise and fall to increase during this transition. This observation suggests that turbulent transport could play an important role in the plasma behavior around the density limit. The magnetic field dependence in the Sudo scaling should suggest the relation between the turbulent transport and density limit, i.e.,  $n_{\text{limit}} \propto \sqrt{B}$ .

## 2.3 Attractive confinement regimes in stellarators

Recent studies in stellarators have found many interesting operational regimes, such as super dense core (SDC) in LHD [9, 10]. In the SDC discharge, the achieved density is  $4.5 \times 10^{20} \text{ m}^{-3}$  with electron temperature of 0.85 keV. This is attained with a series of pellet injections. Besides, the high density H (HDH) mode was found in W7-AS [11–13] where the density up to  $4 \times 10^{20} \text{ m}^{-3}$  is sustained in a rather stationary manner.

As is shown in Fig. 3 (a), the extremely sharp gradient is created in the density profile at the plasma edge. In contrast to usual H-mode in tokamaks, the HDH-mode is that the transition happens above a critical density. Another special feature with the HDH-mode is the favorable reduction of impurity confinement. As is shown in Fig. 3 (b), the impurity confinement time is sharply deteriorated above the critical density, while the bulk particle confinement is clearly enhanced. Similar behavior of carbon impurity is found in LHD, or the outward move-

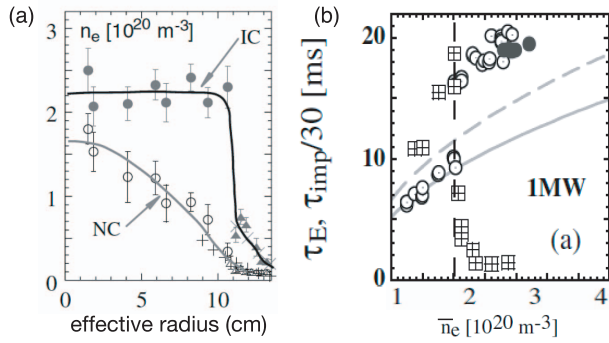


Fig. 3 HDH mode discovered in W7-AS. (a) The comparison between density and temperature profiles in normal confinement (NC) and improved confinement (HDH) mode. (b) The difference between confinement times of NC and HDH mode. The squares indicate the impurity confinement time.

ment of carbon is observed when high toroidal rotation of plasma is induced by higher power of neutral beam injection (NBI) [14]. This feature is an advantage because spontaneous ash-removal can be expected if this phenomenon is valid for helium ions.

### 3. Transport and New Paradigm

#### 3.1 Collisional transport and symmetry

The transport in magnetically confinement plasma is described as the total of collisional and turbulent transport. The diffusive coefficient of collisional process is generally expressed as  $D \propto \Delta^2 \nu_{ei}$ , where  $\Delta$  and  $\nu_{ei}$  are the effective step width and collision frequency, respectively. The effective step width is related with the deviation of a particle orbit from the magnetic field flux surface, and can be large if the collisionality is sufficiently low to allow the particles to be trapped in the magnetic field mirror associated with the inhomogeneity of the confinement magnetic field. Therefore, the effective step width is a function of collisionality and geometrical property of confinement field.

In tokamaks, the poloidal inhomogeneity of the magnetic configuration gives birth to the particles trapped in poloidal mirror field, termed banana particles. The existence of banana particles enhances the collisional transport. On the other hand, non-axisymmetric (or three dimensional) configurations of stellarators produce the other kind of trapped particles, so-called helically trapped particles, to enhance the collisional transport. Therefore, the superiority of stellarators in steady state operation can be accompanied with the inferiority in collisional transport without any optimization of the magnetic field configuration [15].

#### 3.2 Bipolar diffusion and barrier formation

Confinement improvement, in addition to steady state operation, is a critical issue in order to realize a more economic reactor. The stellarators could provide a compatible

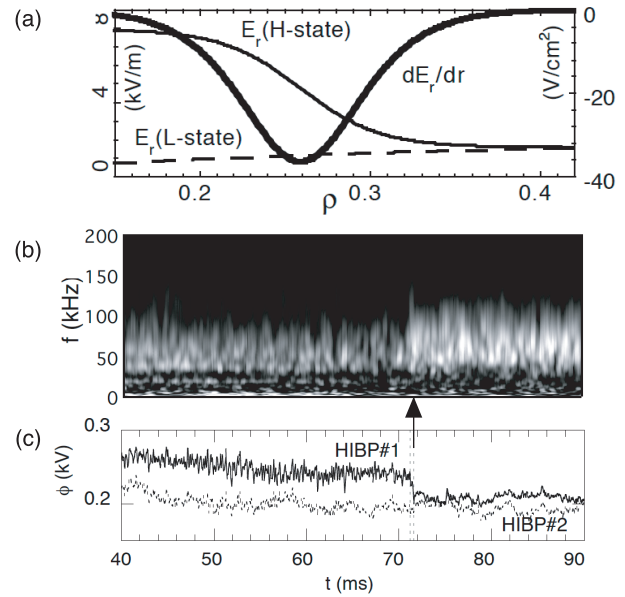


Fig. 4 The property of transport barrier in stellarator. (a) The profiles of radial electric field and its shear around the ITB in CHS. (b) Electric field fluctuations at the barrier before and after the collapse of the barrier, and (c) potential drop inside the barrier indicating the collapse of the barrier, together with the potential outside.

solution to realize the improvement of turbulence driven transport and steady state operation. It is known that the bipolar diffusion due to helically trapped particles should be the dominant process to form the radial electric field in stellarators. The radial electric field in a steady state should be determined by the balance between collisional ion and electron fluxes denoted  $\Gamma_{ion}(E_r)$  and  $\Gamma_{electron}(E_r)$ , respectively, i.e.,  $\Gamma_{ion}(E_r) - \Gamma_{electron}(E_r) = 0$  in stellarators, while the generation mechanism of radial electric field is still an open question in tokamaks. Moreover, the nonlinear dependence of collisional fluxes on radial electric field causes the bifurcation nature of radial electric field in stellarators [16, 17].

This bifurcation nature of radial electric field with stellarators has been found to be the cause of internal transport barrier (ITB) commonly observed in stellarators [18–21]. The formation scenario is identical with the model proposed for the explanation of H-mode initially [22, 23]. In a stellarator plasma core where temperature is above a critical value, the radial electric field makes a transition into a strongly positive branch (or electron root) with the radial electric field outside still remaining in a weakly positive branch (or ion root). As is shown in Fig. 4(a), the transition creates the transient layer between the two branches. The rather large electric field shear is produced in the layer to reduce the turbulence and form the transport barrier according to the  $\mathbf{E} \times \mathbf{B}$ -shearing of turbulence [24–28].

On the other hand, as is shown in Fig. 4(b), the sudden increase in fluctuation is observed in the connection

layer or the position of the ITB after the back-transition indicated by the sudden drop of potential (Fig. 4 (c)). The observed transition time scale of radial electric field is in the range of a few dozen microseconds, being consistent with that prediction of the neoclassical theory [29]. The time scale is much faster than the confinement time scale, therefore, this means that the existence of multi-steady states of electric field.

Accordingly, the ITB in stellarators is an exceptionally clear example to demonstrate that the electric field bifurcation can be the cause for the barrier formation. In contrast the formation of the H-mode or edge transport barriers both in tokamaks and stellarators still allows of many candidate mechanisms; some experimental results suggest the balance between fast ion loss and parallel viscosity, while some others suggest the turbulent Reynolds stress should play an important role. The non-axisymmetric feature, instead of the anxiety of collisional transport, could give stellarators an advantage in the transport barrier formation, of which cause is clearly identified thus theoretically predictable rather easily.

### 3.3 Zonal flows and new paradigm

The magnetic well and shear have been known to be the concepts to measure the magnetic configuration property to stabilize the linear MHD and drift wave instabilities. Therefore, these concepts have been used as the major factors to optimize the magnetic field configuration. The recent development of theories and plasma diagnostics also has shown a new paradigm [30, 31], which could be common for magnetically confined plasmas, to understand the saturation mechanisms of the plasma turbulence and the resultant transport. In other words, the new paradigm can be a new factor to evaluate the property of the magnetic field configuration in terms of turbulent saturation mechanism, while the magnetic shear and well serves as the factors to

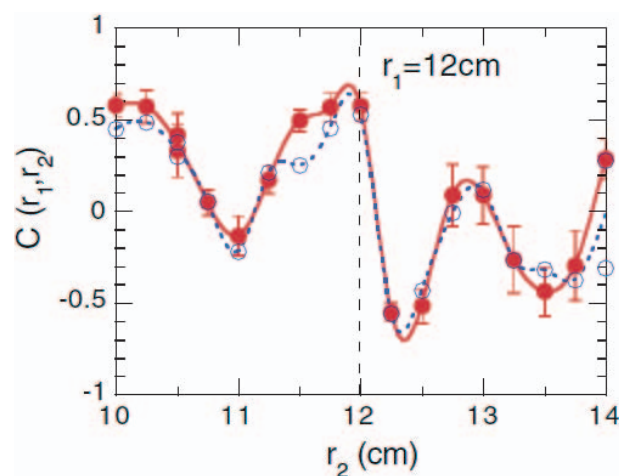


Fig. 5 The identified radial pattern of zonal flows in CHS. The radial structure of zonal flows is represented in the radial correlation function.

assess the linear growth of the instabilities [32, 33].

In the new paradigm, the turbulence should be recognized as a system of zonal flows and drift waves. Inhomogeneity of plasma (i.e., temperature and density gradients) causes drift wave turbulence to result in the enhancement of plasma transport. Then the drift waves generate and transfer the energy to zonal flows through the  $v\nabla v$ -nonlinearity. Moreover, the zonal flows give back-reactions on the drift waves, such as  $\mathbf{E} \times \mathbf{B}$ -shearing, wave trappings, and so on, to work as further reduction of drift-waves. The symmetric nature of zonal flows causes no radial or cross-field transport. Therefore, the increase in the zonal flow fraction in the turbulence contributes to lessen the anomalous transport. The fraction of zonal flows in the power spectrum of electric field fluctuations, therefore, is a key to determine the turbulent transport level.

The direct measurements of electric field fluctuations in CHS have proven the existence of zonal flows experimentally, together with the couplings between zonal flows and the background turbulence [34–36]. A number of experimental reports have been accumulated to show the existence of Geodesic Acoustic Modes (GAMs), an oscillatory branch of zonal flows [31], and their couplings with the background turbulence [37] using direct and indirect measurements of flow or electric field. Therefore, the new paradigm of plasma turbulence and transport is widely prevailed nowadays. Figure 5 shows the radial correlation function between the electric field fluctuations corresponding to the stationary zonal flows, visualizing the radial pattern of zonal flows.

### 3.4 Confinement and flow damping rate

The essential requirement for detecting the zonal flows is to measure the fluctuations of plasma flows or electric field directly. This imposes a quite difficult constraint on the present plasma diagnostics, therefore, limited data have been available. However, the comparison between fluctuation spectra of flow (or electric field) in tokamak and stellarator is possible. Figure 6 shows the electric field spectra directly measured with HIBPs in the core of CHS

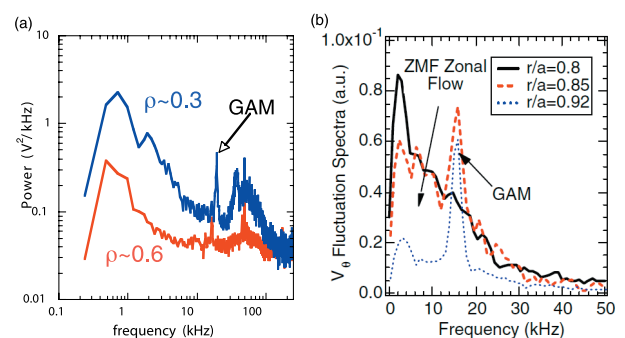


Fig. 6 The comparison between spectra of (a) electric field fluctuations measured with HIBP (CHS), and (b) poloidal flow fluctuations measured with BES (DIII-D).

stellarator, and the flow fluctuation spectra indirectly measured with BES in the edge region of DIII-D tokamak [38].

In spite of the difference of magnetic field configuration and the observed locations, the comparison shows the common features, i) a region corresponding to stationary zonal flows exists, ii) the oscillatory branches, GAMs, are observed as sharp peaks, and iii) regions with broad band fluctuations corresponding to drift waves with a higher frequency from a few dozen kHz to a hundred kHz are present. In the case of CHS stellarator, the fraction of turbulent power increases being accompanied with the increase of zonal flow fraction to that of the drift waves around  $\sim 50$  kHz, probably due to the enhancement of temperature gradient in the plasma core region. In the case of DIII-D tokamak, the GAM fraction decreases with an increase in zonal flow amplitude as the observation point goes inward.

It has been found that the absolute value of GAM amplitude should be much larger in tokamak than in stellarator. The HIBP observations in JIPPT-IIU [39] showed that the GAM potential amplitude can exceed  $\sim 100$  V, while that in CHS stellarator should be in the range of a few volts. This may be ascribed to the larger parallel viscosity of stellarators. Figure 7 shows the comparison between toroidal flows driven by NBI in stellarator (CHS) and tokamak (JFT-2M). Obviously, the resultant toroidal rotation velocity in tokamak is much faster than that in stellarator, although the input NBI power is in the same range in both experiments of CHS [40] and JFT-2M [41]. Thus, the inhomogeneity should give a large damping effect on plasma flows.

As for the ITB in stellarator, the transport inside the barrier is also found to be improved without any significant electric field shear. Recently, it has been confirmed in CHS that this improvement is caused by the enhancement of zonal flow fraction, as is shown in Fig. 8, due to the reduction of flow damping rate [42, 43]. The zonal flows (or zonal radial electric field) are driven by turbulence, therefore, the turbulent radial current to drive the zonal flows,  $\delta j_{\text{turb}}$ , should be balanced with the neoclassical radial current (or total radial flux of ions and electrons) in stellarators, this condition is expressed as  $\delta j_{\text{turb}} + (\partial j_{\text{neo}} / \partial E_r) \delta E_r = 0$ , where  $(\partial j_{\text{neo}} / \partial E_r)$  could be called the effective neoclassical viscosity. The low effective viscosity in electron root is experimentally confirmed, as is shown in the inset of Fig. 8, in addition to the prediction by neoclassical collisional transport theories.

These facts suggest that the zonal flow fraction should be large as the flow-damping rate is low. Hence, the magnetic field configuration with lower parallel viscosity or magnetic inhomogeneity should give a better confinement owing to the possible enhancement of zonal flow fraction. The new paradigm could provide an optimization principle for the magnetic field configuration in the light of turbulence transport by its saturation mechanism.

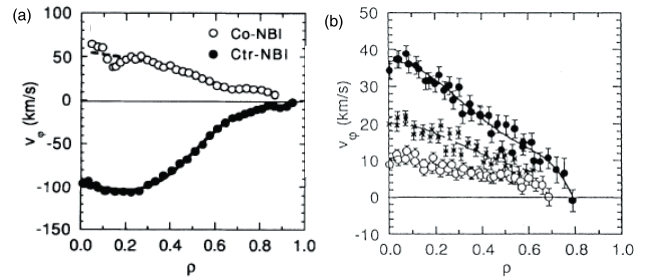


Fig. 7 The comparison between induced toroidal flows in tokamak (JFT-2M) and stellarator (CHS). (a) The profile of toroidal flow velocity in JFT-2M and (b) that in CHS. The toroidal flows are measured with charge exchange recombination spectroscopy.

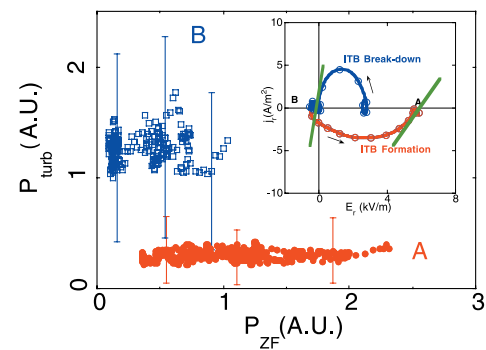


Fig. 8 The fluctuation power of drift waves as a function of that of zonal flows for the state with and without confinement improvement in CHS. The measurement was carried out at a point inside the position of ITB. The increase in zonal flow power should be ascribed to the decrease in effective viscosity accompanied with the transition from ion (point B) into electron root (point A). The effective viscosity corresponds to the slope of the tangential lines at the stable points of radial electric field in the inset. It is clear that the slope of ion root is steeper than that of electron root solution.

## 4. Beyond Simple Comparison

### 4.1 Roles of low temperature devices

High accessibility and flexibility must be of essential need for the experiments aiming at finding the physical laws underlying the structural formation of plasmas. The role of low temperature devices should be emphasized in addition to exploring new possible diagnostics for high temperature plasmas. Low temperature devices, even a linear cylindrical device, provide good environments to study the fundamental processes of plasma turbulence and transport.

For instance, in low temperature toroidal device, H1-heliac, the fundamental processes of plasma turbulence has been extensively studied [44, 45]. In TJ-K the dependence of turbulence characteristics on dimensionless parameters, such as normalized Larmor radius,  $\rho^*$ , collisionality  $\nu^*$ , and so on, has been pursued for the first principle understanding of the dimensionless scaling law of plasma confine-

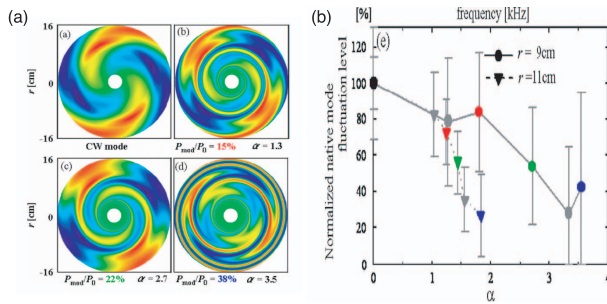


Fig. 9 Observation to demonstrate the interplay between the sheared flows and a pressure driven mode in a linear cylindrical plasma. The sheared flow strength is controlled by the degree of the modulation of ECR-heating. (a) The reconstructed images of the interplay between sheared flows and the mode. (b) The suppression degree as a function of a parameter to indicate the shear flow strength,  $\alpha$ .

ment [46]. The simultaneous measurements of both radial and poloidal wavenumbers using 2-dimensional probes in TJ-K succeeded in clarifying the fundamental process of magnetized plasma turbulence, i.e., the nature of dual cascade in a two dimensional flow system [47].

Besides, a number of excellent experimental results have been reported from cylindrical linear devices in university laboratories. In CSDX, a cylindrical laboratory plasma, the momentum balance between the turbulent Reynolds stress drive and viscous damping was investigated and successfully demonstrated that the zonal flow Reynolds stress should be the cause of the zonal flow generation [48]. In a cylindrical machine, LMD-U, the streamer formation has been identified with an efficient use of the combination of 64 channel azimuthal probe array and 2 dimensionally movable probes [49].

Recently, In a laboratory cylindrical plasma of Kyushu university, the detailed processes of sheared flow effect were observed in externally induced sheared flow using the modulation of the plasma heating power [50]. In the device, a pressure-driven instability is observed in electron cyclotron heated plasma as a sharp peak without any modulation of ECR-heating. By applying the ECR-heating modulation, the sheared flows are induced to interact with and suppress the native mode. Figure 9 shows the images of the change of the reconstructed potential fluctuation patterns according to the modulation intensity of heating power, and the suppression ratio of the native mode as a function of the strength of the induced sheared flow. The results clearly demonstrate how the native mode is altered as the shear flow becomes stronger, suggesting that the process of three wave coupling should play a role in the suppression.

## 4.2 Concluding remarks

Tokamak is the leading concept for fusion reactor, however, it is necessary to overcome a number of issues for

realizing an economically compatible reactor. The advantageous properties of the other toroidal devices, therefore, should be incorporated into a Demo and following reactors; for instance, the advantage with stellarators, the high density operation exceeding the Greenwald limit without any disruptive activities, would be desired to be adopted to the tokamak concept even though the axisymmetric nature giving a good plasma confinement may be partially destroyed. In order to realize a device with a combined concept or an optimizing configuration, it is absolutely essential to understand the plasma behavior to determine the operational boundaries and the plasma confinement from the first principle, which should result in the precise and accurate prediction of magnetically confined plasma performance to any given configurations. Therefore, the important roles of medium and small sized devices oriented for physical understanding of toroidal plasmas are strengthened even in the era of burning plasmas.

- [1] M. Gryaznevich *et al.*, Phys. Rev. Lett. **80**, 3972 (1998).
- [2] M. Murakami *et al.*, Nucl. Fusion **16**, 347 (1976).
- [3] M. Greenwald *et al.*, Nucl. Fusion **28**, 2199 (1988).
- [4] D.L. Brower *et al.*, Phys. Rev. Lett. **67**, 200 (1991).
- [5] S. Sudo *et al.*, Nucl. Fusion **30**, 11 (1990).
- [6] J. Miyazawa *et al.*, Nucl. Fusion **48**, 015003 (2008).
- [7] B.J. Peterson *et al.*, Nucl. Fusion **41**, 519 (2001).
- [8] L. Giannone *et al.*, Plasma Phys. Control. Fusion **42**, 603 (2000).
- [9] N. Ohya *et al.*, Phys. Rev. Lett. **97**, 055002 (2006).
- [10] R. Sakamoto *et al.*, Nucl. Fusion **46**, 884 (2006).
- [11] K. McCormick *et al.*, Phys. Rev. Lett. **89**, 015001 (2002).
- [12] F. Wagner *et al.*, Plasma Phys. Control. Fusion **48**, A217 (2006).
- [13] M. Hirsch *et al.*, Plasma Phys. Control. Fusion **50**, 053001 (2008).
- [14] K. Ida, M. Yoshinuma, M. Osakabe *et al.*, Phys. Plasmas **16**, 056111 (2009).
- [15] H.E. Mynick, Phys. Plasmas **13**, 058102 (2006).
- [16] L.M. Kovrizhnykh, Nucl. Fusion **24**, 435 (1984).
- [17] D.E. Hastings, Phys. Fluids **27**, 935 (1984).
- [18] A. Fujisawa *et al.*, Phys. Rev. Lett. **82**, 2669 (1999).
- [19] U. Stroth *et al.*, Phys. Rev. Lett. **86**, 5910 (2001).
- [20] A. Fujisawa, Plasma Phys. Control. Fusion **45**, R1 (2003).
- [21] M. Yokoyama *et al.*, Nucl. Fusion **47**, 1213 (2007).
- [22] S.-I. Itoh and K. Itoh, Phys. Rev. Lett. **60**, 2276 (1988).
- [23] K.C. Shaing and E.C. Crume Jr., Phys. Rev. Lett. **63**, 2369 (1989).
- [24] K.C. Shaing *et al.*, *Proceedings of 12th International Conference on Plasma Physics and Controlled Nuclear Fusion Research*, Nice, 1988 (International Atomic Energy Agency, Vienna, 1989) Vol.2, p.13.
- [25] H. Biglari *et al.*, Phys. Fluids B **2**, 1 (1990).
- [26] K. Itoh *et al.*, Plasma Phys. Control. Fusion **36**, 123 (1994).
- [27] T.S. Hahm and K.H. Burrell, Phys. Plasmas **2**, 1648 (1995).
- [28] Z. Lin *et al.*, Science **281**, 1835 (1998).
- [29] A. Fujisawa *et al.*, Phys. Rev. Lett. **79**, 1054 (1997).
- [30] P. H. Diamond *et al.*, Plasma Phys. Control. Fusion **47**, R35 (2005).
- [31] A. Fujisawa *et al.*, Nucl. Fusion **47**, S718 (2007).
- [32] J. Nührenberg and R. Zille, Phys. Lett. **114A**, 129 (1986).
- [33] J. Nührenberg and R. Zille, Phys. Lett. **129**, 113 (1988).

- [34] A. Fujisawa *et al.*, Phys. Rev. Lett. **93**, 165002 (2004).  
[35] A. Fujisawa *et al.*, Plasma Phys. Control. Fusion **49**, 211 (2007).  
[36] A. Fujisawa *et al.*, J. Phys. Soc. Jpn. **76**, 033501 (2007).  
[37] Y. Nagashima *et al.*, Phys. Rev. Lett. **95**, 095002 (2005).  
[38] D.K. Gupta *et al.*, Phys. Rev. Lett. **97**, 125002 (2006).  
[39] Y. Hamada *et al.*, Nucl. Fusion **45**, 81 (2005).  
[40] K. Ida *et al.*, Phys. Rev. Lett. **67**, 58 (1991).  
[41] K. Ida *et al.*, Phys. Rev. Lett. **68**, 182 (1992).  
[42] K. Itoh *et al.*, Phys. Plasmas **14**, 020702 (2007).  
[43] A. Fujisawa *et al.*, Phys. Plasmas **15**, 055906 (2008).  
[44] M.G. Shats *et al.*, Phys. Rev. E **71**, 046409 (2005).  
[45] H. Xia, M.G. Shats and H. Punzmann, Phys. Rev. Lett. **97**, 255003 (2006).  
[46] U. Stroth *et al.*, Phys. Plasma **11**, 2558 (2004).  
[47] P. Manz *et al.*, Plasma Phys. Control. Fusion **50**, 035008 (2008).  
[48] G.R. Tynan *et al.*, Plasma Phys. Control. Fusion **48**, S51 (2006).  
[49] T. Yamada *et al.*, Nature Phys. **4**, 721 (2008).  
[50] H. Tsuchiya *et al.*, Plasma Phys. Control. Fusion **50**, 055005 (2008).